RJC

RASĀYAN *J. Chem.*
Vol. 18 | No. 1 |295-303| January - March | 2025
ISSN: 0974-1496 | e-ISSN: 0976-0083 | CODEN: RJCABP
http://www.rasayanjournal.com
http://www.rasayanjournal.co.in

SYNTHESIS, STRUCTURAL CHARACTERIZATION, DFT AND DOCKING STUDIES OF 4, 5- DIPHENYL-1-(2 (PYRROLIDIN-1-YL)-ETHYL-2 (P-TOLYL)-1H-IMIDAZOLE

S.M. Anuradha[1,✉], P. Ezhilmathi[2] and K. Anbarasu[1]

[1]Department of Chemistry, Thiru Kolanjiappar Government Arts College, Virudhachalam-606001, Affiliated to Annamalai University, Chidambaram, Tamilnadu, India
[2]Department of Chemistry, Jawahar Science College, Neyveli-607803, Affiliated to Annamalai University, Chidambaram, Tamilnadu, India
✉Corresponding author: anuradhapac@gmail.com

ABSTRACT

A novel crystal compound of 4,5-Diphenyl-1-(2-(pyrrolidin-1-yl)- ethyl-2(p-tolyl)-1H-imidazole (DPEI)inventive is experimentally calculated by FT-IR and FT-Raman. The compound affirmed sole crystal XRD investigation and upgraded bond parameters were computed hypothesis (DFT) at B3LYP/6-311++G (d,p)—the enhanced acquired by DFT calculations appreciable tolerance sole gem XRD information. The HOMO-LUMO exhibit conveys conjugation deep in the particle. Molecular Electrostatic Potential (MEP) guides the most reactive site. The synthesized target molecule (DPEI) is a latent NLO material since it has 18 times higher $\mu\beta_0$ value than the standard. The obtained glide score value (-5.987kcal/mol) indicated the survival of effective reciprocal action between the DPEI molecule and the 1X02 anticancer protein. The cytotoxicity effect of the DPEI molecule against HepG2 (liver cancer cell line) revealed that the target molecule is a better candidate for the anti-cancer activity.

Keywords: Single crystal, XRD, Docking, and NLO.

RASĀYAN*J. Chem.*, Vol. 18, No.1, 2025

INTRODUCTION

Imidazole is a category of exceedingly five-membered ring, it establishes numerous legitimate things and pharmacore[1-2]. The imidazole derivatives manifest fluorescence properties and erosion conservation belongings on lenient steel[3-4]. The multidentate imidazole-based polymers are prepared from a modern erratic treble polymerization system[5]. Imidazole imitative exhibits linear and nonlinear photophysical properties.[6-7]The imidazole is eventually utilized as a dopant for doping organic semiconductor materials and used as π- conjugated backbone in charge-transfer chromospheres[8-9]. The imidazole consequent HOMO-LUMO energy space results were revealed to be used in the solar energy conversions[10-14]. The DFT studies of imidazole indicated inter and intra-molecular hydrogen bonds exhibited in the crystal systems[15]. In many of the metal complexes, imidazole eventually acts as a ligand[16]. Imidazole imitative possesses assorted therapeutic pursuits *viz.*, anti-viral[17] anti-malarial[18], anti-plasmodial, and plasmepsin prohibition[19]. Nitro-substituted imidazole eventually persists as FabH inhibitors and thiazole substituted imidazole imitative are used as inhibitors of 15-lipoxygenase[20-21], cholinesterase inhibitors[22], anti-Alzheimer's diseases[23], chromogenic properties, and anti-leishmanial activity[24-25]. Several novel drugs perceived for the reception of cancer and imidazole eventually also have potent anticancer activities[26]. N-substituted pyrrolidines are utilized in the consideration of anti-convulsant[27], antimicrobial, anti-HIV, and Nucleocapsid protein inhibitors[28]. Vibrational spectral analysis is a profitable device for the illumination of an anatomy. Vibrational spectroscopy has proven a valuable contributor in the diverse fields of science to the analysis of first-order hyper polarizability and NBO properties[29-30].

EXPERIMENTAL

General Methods

FT-Raman analysis investigation was conveyed from an innovator instrument facility (LABRAM-HR) with laser excitation lines of 514nm at normal temperature. IR spectrum was recorded in a Thermo Nicolet spectrometer. All the chromatographic refinement was executed with silica gel laminated (Merkiesel 60GF,

0.2mm thickness) plates. The pure starting materials and solvents were secure from Sigma-Aldrich and Alfa Aesar and X-ray crystallographic interpretation was executed using Bruker SMART APEXCCD instrument. The molecular docking assay was conveyed with GLIDE- Schrödinger Software.

Synthesis of 4, 5-diphenyl-1-(2 (pyrrolidin-1-yl) ethyl-2-(p-tolyl)-1-H imidazole

An interfusion of 1-(2-amino ethyl pyrrolidine) (1mmol), aromatic para-substituted aldehyde (1mmol), benzil (1mmol), and ammonium acetate (2mmol) with SO_4^{2-}/Y_2O_3 (30mg) as speed up the reaction in the acetic medium. All the species were taken in a spherical bottom flask and the reaction composition was made hot up to 80^0C in ethanol. The reaction progression was investigated by TLC with a solvent ratio of 8:2 (Pet ether: Ethyl acetate) as the eluent. The reaction combination of deracinating with chloroform and the ramification liquid was rectified by chromatographic techniques.

Spectral Data of DPEI Molecule:4, 5-diphenyl-1-(2-pyrrolidin-1-yl) ethyl-2-(p-tolyl)-1H-imidazole

Yellow crystalline rigid: m.p.120ºC and yield 94%. IR (KBr) (cm^{-1}): 2758-3438 (C-H) 1607 (C=N) 1528, 1499, 1481, 1440(C=C stretching). ^{1}H NMR(δ ppm):1.25 (S,4H), 1.588 (S,4H protons), 2.39 (t,2H), 4.03 (t,2H), 2.13 (3methyl protons), 7.1-7.6 (m,14H aromatic protons), ^{13}C NMR (δ ppm): 21.42 (C-4), 23.32 (C-4), 43.60 (C-2 carbon), 55.70 (C-2 carbon), 53.95 (methyl carbon), 147.92 (C=N carbon), 126-138 aromatic carbons, displayed in Fig 1c and 1d.

DFT Computational Method

The Gaussian 03W package adequate to enumerate the Raman bustle[31], NLO, NBO analysis, Mulliken atomic charge, and thermodynamic equity are enumerated. The discursive theoretical calculations on the molecular frame the creation of metal-ligand bonding, vibrational frequencies, and emphasis were executed by utilizing different DFT techniques, cross-breed (PBEO, mpw1pw, and B3LYP) various effective core potentials (ECP) are acclimated[32] Raman spectrum explains the respective molecule, vibration mode of each peak, charge transfer and surface enhancement can be determined[33].

X-ray Crystallographic Analysis

The crystal was developed by gradual disposal routine in sheer solvent. The crystal was clarified by explicit methods (SHELXA-97) and delicate sole crystal X-ray diffraction investigation toted out utilizing three circles Bruker SMART APEXCCD and Rigaku Saturn 724 area detector system under $\mu_0 k_\alpha (\lambda=0.71073A^0)$ graphite monochromatic X-ray beam. The structure is confirmed by the supplementary (CCDC number: 1860058).

Molecular Docking Assay

Molecular docking is a technique that speculates the favored coordination of specific molecule when caper in an effective site of further molecule to form a fixed complex such that the spontaneous energy of the universal strategy is diminished. The 3D framework of 1X02 was used. The perfect docking miniature was selected as stated in the minimum mandatory energy determined by Schrödinger and the better fitting imperative configuration was performed by aqua phobic interactions.

Cytotoxicity Effect of DPEI Molecule: Cell Culture and Treatment with Compounds

HepG2 cells ensure a DMEM medium accessory with 11% thermal immobilized fetal calf serum at 37 °C, and 5.5% CO_2 for 24 h previous measurement. Cells existed for interior investigations to establish eight pathways for the fortification of cell lines. The DMSO congregation remained constant at 0.55% (v/v). HepG2 cells persist implanted in an acculturing dish and split into three groups in the usual methods compounds supplemented at 0, 1.85, 3.8, 7.7, 15.5, 31.2, 62.4, 125.1, 250.0, and 500 mg/L. everyone's specimen holds at least three reproduce. Cells occur again cultivated for 24.5, 48.5, or 72.5 h separately.

Determination of Cytotoxicity

Mitochondrial functions tetrazolium moiety (MTT) to formazan was used as an estimate the cell survivance[34]. HepG2 plasma laminate probity was measured by investigating lactate dehydrogenase (LDH) leakage into the cultivation medium[35]. The synthesized imidazole moiety estimation of cytotoxicity by MTT assays was executed at four concentrations, 1.83, 3.73, 7.63, 15.53, 31.23, 62.42, 125.1, 250.0, and 500 mg/L respectively.

RESULTS AND DISCUSSION

Crystal and Molecular Structure of 4,5-diphenyl-1-(2(pyrrolidin-1-yl)-ethyl-2(p-tolyl)-1H-imidazole [DPEI]

Specific sole X-ray ramification investigation of execute for 4, 5-diphenyl-1-2(pyrrolidine-1-yl)–ethyl-2(p-tolyl)-1H imidazole (DPEI) and its translucent, structure refining. The ORTEP diagram illustrates the DPEI molecule exhibited in Fig.-1 & 2. The sole crystal data is a=10.0372(2) A^0, b=14. 863(4) A^0 c=15.314(4) A^0. The observed bond length of the imidazole loop C=N is 1.321A^0. It is larger than the normal C=N value and lower than the C-N (1.47A^0) bond distances concluding the effective electron delocalization occurring in the imidazole girdle. In the imidazole core structure, the C10-N9 bond length is 1.386 and the C8-N9 bond length is 1.36 A^0. These C-N bond distance values are lower than the C14-N15 bond distance (1.441A^0) confirming the involvement of effective delocalization in the imidazole loop. The C26-C11-C10-C20 dihedral angle value is almost equal to zero conceding that the two phenyl rings exist in the planar orientation. The dihedral angle value of N9-C13-C14-N15 is 162.7A^0conformsto the pyrrolidine moiety existent in the out-of-plane from the imidazole loop. Table-1 and the values indicated that all the experimental values are proficient in concurrence with the theoretical values. The observed dihedral angle values C_8-N_{12}-C_{11}-C_{26}(-179.8A^0), H_{30}-C_{30}-C_{29}-C_{23}(179A^0), $C_{31}C_{30}C_{29}H_{29}$ (179.61A^0),H_{30}-C_{30}-C_{31}-C_{26} (179.9A^0), C_{29}-C_{30}-C_{31}-H_{31}(179.9A^0), H_{29}-C_{29}-C_{28}-C_{27}(179.8A^0), C_2-C_7-C_6-H(-179.6A^0),H_7-C_7-C_6-C_5 (179A^0), H_{22}-C_{22}-C_{23}-C_{24}(179A^0), C_{21}-C_{22}-C_{23}-H_{23}(179.8A^0), H_{22}-C_{22}-C_{21}-C_{20}(-179.7A^0), C_{23}-C_{22}-C_{21}-H_{21} (179.6A^0), C_{23}-C_{24}-C_{25}-H_{25} (179.9A^0) confirmed the planar orientation of the phenyl rings. The packing diagram in Fig.-3. indicates that eight molecules exist in the unit cell.

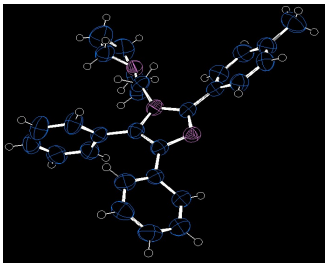

Fig.-1: ORTEP Diagram of Imidazole Crystal Moiety

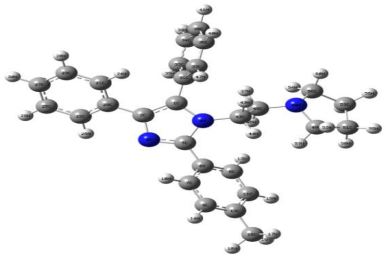

Fig.-2: The Optimized Molecular Structure of Imidazole Crystal Moiety

Table-1: Selected Bond Distance, Bond Perspective,and Torsional Angle of 4, 5 diphenyl-1-(2(pyrrolidin-1-yl) ethyl-2-(p-tolyl)-1H- imidazole [DPEI]

Parameters	4, 5-Diphenyl-1-(2(pyrrolidin-1-yl) ethyl-2-(p-tolyl)-1H- imidazole.
Stoichiometric formula	C28H29N3
Molar mass	407.54
Fahrenheit, K	293(2)
Wavevector, λ	0.71073A^0
Space lattice	Monoclinic, P21/c
Small space place	a = 10.037(2) Å α = 90.
	b = 14.863(4) Å β = 95.746(7).
	c = 15.314(4) Å γ = 90.
Volume, V	2273.1(10) Å3
Z, Calculated density	4,1.191 Mg/m3
F(000)	872
catalog	-12<=h<=13, -14<=k<=19, -19<=l<=19
Final R indices [I>2sigma(I)]	R1= 0.0676, wR2=0.1314
R indices (all data)	R1= 0.1732 wR2=0.169
Absorption quantity	0.07
Diffraction Radiation Type	MoK\a

Diffraction Radiation Wavelength	0.71073
Reflections Collected	5179
Independent reflections	2254
Goodness of fit	1.034
CCDC NO	1860058

Vibrational Analysis

The vibrational spectral investigation of the DPEI (Imidazole moiety) molecule is displayed in Fig.-1a. (FT-IR) and Fig.-1b. (FT-Raman). The Raman absorption band appeared at 2800cm^{-1} due to νC-H vibrations of the aromatic benzene ring. The band at 1491 cm^{-1} is due to ν C-H of methyl group in benzene ring. The C=N and C-N stretching vibrations appeared at 1680 cm^{-1}, 1418 cm^{-1} (Raman) / 1418 cm^{-1} (IR). The alkenes and alkane group of C-H stretching mode in the molecule were observed at 2934 cm^{-1},2803 cm^{-1} (IR) / 2450 cm^{-1} (Raman). The C=C stretching appeared in the sector of 1000 cm^{-1} (Raman) / 1601 cm^{-1}(IR).

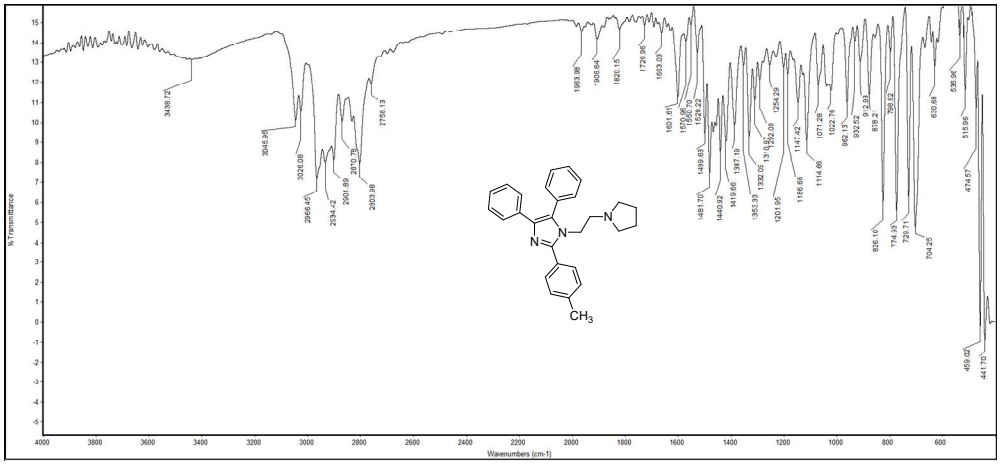

Fig-3: IR Spectrum of Imidazole Moiety

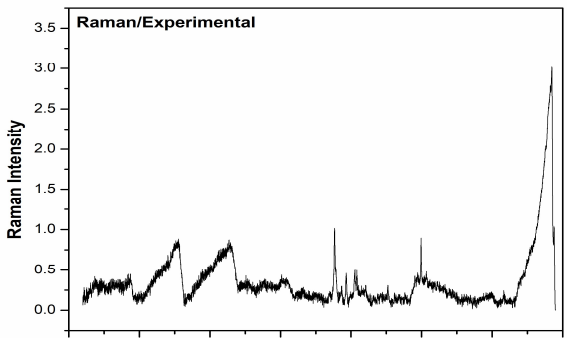

Fig.-4: Raman Spectrum of Imidazole

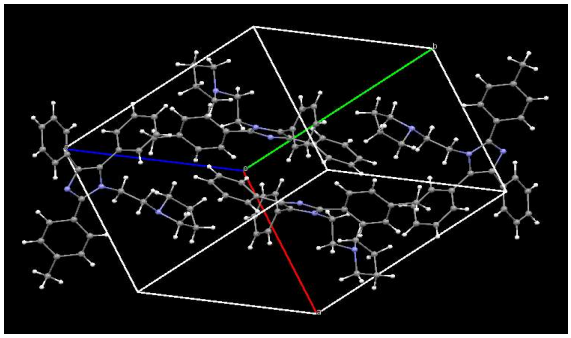

Fig.-5: Packing Diagram of Imidazole Crystal Moiety

HOMO-LUMO Energy

The HOMO-LUMO analysis informed that in the HOMO, the charge density is located up the whole region of the molecule whereas the LUMO part is located more intensively on the imidazole region of the ring system. The potency dissimilarity between the HOMO-LUMO is about 2.821ev explaining the more pliability accuracy DPEI molecule. The HOMO-LUMO energy distance is spare polarizable, with elevated chemical reactivity, and small kinetic stability. The HOMO-LUMO potency designates DPET to acquire superior applicants for electronic applications.

Molecular Electrostatic Potential (MEP)

The MEP diagram imitates electron quantity and the surface illustrates the amount, frame, charge density, and chemical sensation of the molecule. The electrostatic probable of the surface has been indicated by

various colors. The blue shade indicates the lower electron density and the red shade indicates the electron-rich regions.[36]In the DPEI compound the red color concentrated over the nitrogen atom of the imidazole and pyrrolidine ring systems.

Mulliken Atomic Charges

These calculations delineate charges and individual atoms in the molecule. The negative charges are distributed on the nitrogen atom of the imidazole moiety (N3=-0.5509 a.u & N4= 0.5401 a.u) and pyrrolidine moiety (N48=-0.447) whereas positive charges are located more effectively on the C1 atom (C1=O.1750) as displayed in Fig.-4. and Table-2.

Table-2: The Mulliken Atomic Charges of Imidazole Moiety

Atoms	Charges	Atoms	Charges
1C	0.17494	31C	-0.084
2C	0.14528	32C	-0.1268
3N	-0.5509	33C	-0.0487
4N	-0.5401	34C	-0.1071
5C	0.41863	35H	0.19209
6C	0.09868	36C	-0.2696
7C	-0.1105	37H	0.22311
8C	-0.1264	38C	-0.0295
9C	-0.1183	39H	0.07996
10H	0.1158	40H	0.08804
11C	-0.1313	41H	0.08987
12H	0.08783	42C	-0.0238
13C	0.10767	43H	0.1504
14H	0.08445	44H	0.10476
15H	0.07677	45C	-0.0245
16C	-0.3755	46H	0.1074
17H	0.13131	47H	0.03993
18H	0.1182	48N	-0.447
19H	0.11572	49C	-0.0251
20C	0.03614	50C	-0.0744
21C	-0.1207	51C	-0.2101
22C	-0.1114	52H	0.1027
23C	-0.1164	53C	-0.1826
24H	0.14324	54H	0.08976
25C	-0.0971	55H	0.11347
26H	0.10659	56H	0.12913
27C	-0.0775	57H	0.08724
28H	0.08447	58H	0.10448
29H	0.08222	59H	0.09605
30H	0.0784	60H	0.1248

Nonlinear Optics [NLO]

The novel organic nonlinear visual crystals predict the following applications *viz*, optical switching, optical disk data storage, depository optical modulation, discover the isolated area using laser and sticks pharmacological diagnostics.[37] The deliberate hyperpolarizability of the imidazole moiety (β_0=5.56555×10^{30} esu) is nearly 18 times higher than the principal urea ($\beta_{0=}$ 0.3728×10^{-30} esu). Hence deduce that imidazole crystal moiety can exhibit extreme NLO activity.

Thermodynamic Properties

The thermodynamic estimations are one of the parameters used to calculate the energy state of the crystal moiety. At various temperatures for minimum temperature translational energy is maximum in this state the entropy of the system also increases. The other energies like vibrational and rotational energies are minimal in this state.[38-39]

Molecular Docking Studies

Molecular docking evaluation allocates profitable results and shows protein tact in the form of speculating the attraction and activity of little molecules[40]. The newly synthesized crystal and the structurally relevant

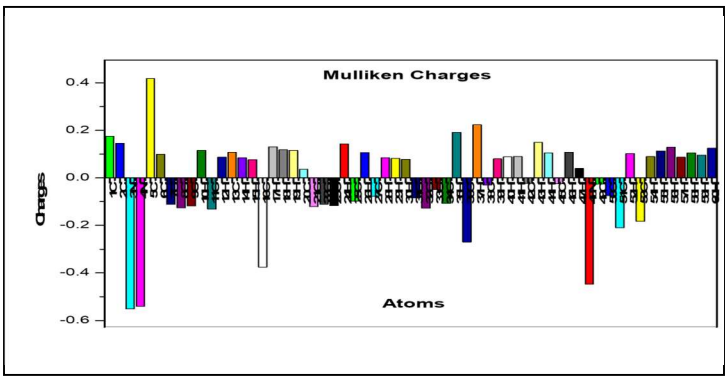

Fig.-6: The Mulliken Atomic Charges of Imidazole Moiety

compounds were subjected toa docking process with anticancer protein (1X02) indicating the best Insilco conformation with the Schrödinger software. Docking of synthesized ligands with 1X02 protein exhibited better interactions and considerable glide score. The crystal molecule 2D and 3D images are displayed in Fig.-5. and docking information is given in the below table. The binding mode of the crystal is effectively bound to 1X02 via hydrophobic, pi-pi staking, pi-cation, and hydrogen bond synergy. Docking investigations and the glide score (-5.98 kcal/mol) affirm that DPEI is the better candidate to act as a prospective anticancer agent. The pharmacokinetic properties of DPEI and related molecules conceded that the DPEI molecules have a better value of blood-brain barrier permeability and a better value of QplogBB.

Lipinski's Rule of Five Factors of Compounds

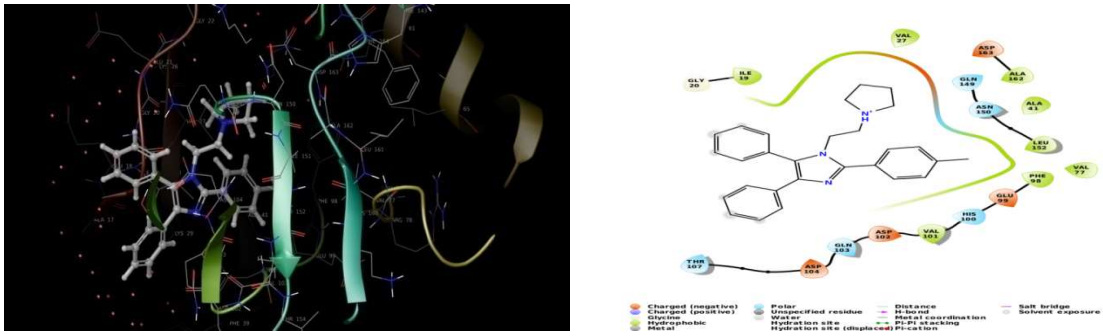

Fig.-7: 2D and 3D View of Binding Interaction of Imidazole Moiety

Cytotoxicity Assay of DPEI Molecule

The synthesized DPEI molecule was tested by resisting the HepG2 cell line and its better activities. The MTT assays were carried out at different concentrations 1.95, 3.9, 7.8, 15.6, 31.3, 62.5, 125.2, 250.1, and 500 mg/L. the standard drug is used as the control. At lower concentrations of DPEI molecules have moderate activity, at higher concentrations they show better activity than the control. Increasing the concentration of DPEI molecules decreases the viability of cancer cells, higher concentration exhibits better activity. The results indicate the crystal molecule exhibits a better cytotoxic effect and also has high cell viability.

CONCLUSION

A newly synthesized crystal imidazole moiety was devoted by the sole crystal X-ray diffraction method. The vibrational assay of the molecule was accomplished by coalescing the empirical and hypothetical information utilizing density functional theory. The HOMO-LUMO strength dissimilarity (2.82087ev) indicates the designated compound has more reactivity, effective conjugation, and good chemical stability.

The NLO property of the DPEI molecule is 18 times better activity than standard urea. The better cooperation of intra-molecular charge shifting was found in the crystal molecule n (LP (1) N4) and π^* C5-N3 with a compensation strength of 81.42 kJ/mol with the electron thickness 0.35ev. Molecular electrostatic potential propounds that the nitrogen bit site (N3and N4) is suitable for electrophilic castigate and the hydrogen bit site (H37) is suitable for nucleophilic attack. Mulliken atomic charge analysis indicated that the C1(0.17494a.u) atom is more positive and the nitrogen atom in the imidazole moiety is (-0.5509 a.u) more negative. The molecular docking investigation and their corresponding glide score (-5.987kcal/mol) indicated that the DPEI molecule has better anticancer activity. The cytotoxicity effect of crystal molecule against HepG2 (liver cancer cell line) moderate to better activity obtained, these results match with the molecular docking assay.

ACKNOWLEDGEMENTS

The authors express their gratitude to Annamalai University for granting permission to conduct this research and to the Department of Chemistry, Thiru Kolanjiappar Government Arts College, Virudhachalam, for providing the necessary facilities to complete this work.

CONFLICT OF INTERESTS

The authors declare that there is no conflict of interest.

AUTHOR CONTRIBUTIONS

All the authors contributed significantly to this manuscript, participated in reviewing/editing, and approved the final draft for publication.The research profile of the authors can be verified from their ORCID ids, given below:

S.M. Anuradha https://orcid.org/0000-0001-6484-5545
P. Ezhilmathi http://orchid.org/0000-0003-0662-0174
K. Anbarasu http://orchid.org/0000-0003-2234-8676

REFERENCES

1. D. A. Shabalin and J. E. Camp, *Organic Biomolecular Chemistry,* **18**, 3950(2020), https://doi.org/10.1039/D00B00350F
2. I.M. Nadeemlone and H.Y.AboulEnein, *Medicinal Chemical Communication*, **8(9)**, 1742(2017), https://doi.org/10.1039/c7md00067g
3. H. Daemi, R.R. Rad, M. Barikani and M. Adib, *Applied Catalysis A*., **468**, 10(2013), https://doi.org/10.1016/J.APCATA.2013.08.023
4. H.V. Tolomeu and Manssour Fraga, *Molecules*, **28(2)**,838(2023), https://doi.org/10.3390/molecules28020838
5. Y. Shen, M.Y. Gee and A.B. Greytak, *Chemical Communications,* **53**, 827(2017), https://doi.org/10.10391cc07998A
6. L. Athishu Anthony, D. Rajaraman, G., Sundararajan, M, Suresh, P. Nethaji, R. Jaganadhan and Kumaradhas Poomani, *Journal of Molecular Structure*, **15,** 1266(2022), https://doi.org/10.1016/j.molstru.2022.133483
7. A. Viswanath, Y. Shen, A.N. Green, A.B. Greytak and B.C. Benicewicz, *Macro Molecules*, **47,** 8137(2014), https://doi.org/10.1021/Ma501955T
8. R. Tan. S.K. Robert, M.Y. Gee, D.A. Blom and A.B. Greytak, *Quantum Dots,* **27**, 7468(2015), https://doi.org/10.1021/ACS.Chemmater.5B03588
9. H.A.Al Ghamdi, F.A.Almughem, M.A.Alshabibi, N.A.Alzahrani, E.A. Tawfik, and L.A.Damiati,*Biomolecules,***9(14)**, 1198(2024), https://doi.org/10.3390/biom14091198
10. S. Ankit and V. Prabhakar Kumar, *BioMedCentral Chemistry,* **12,** 1(2021), https://doi.org/10.1186/S13065-020-00730-1

11. S.A. Salem, A.H. Khazaei, J. Yousefiseyf, N. Sarmasti and M.M. Gilan, *Polycyclic Aromatic Compounds,* **41,** 319(2021), https://doi.org/10.1080/10406638.2019.1582076
12. L. Yin and L. Wang, *Tetraherdon Letters,* **57**, 5935(2016), https://doi.org/10.1016/j.tetlet.2016.11.089
13. M. Mao, X.L. Zhang and G.H. Wu, *International Journal of Photoenergy,* **3**, 268(2018), https://doi.org/10.1155/2018/2061472
14. P. Ezhilmathi, V. Manikandan, V. Revathi and K. Krishnasamy, *Journal of Computational and Theoretical Nanosciences,* **16**, 1512(2019), https://doi.org/10.1166/jctn.2019.8067
15. H.V. Tolomeu, C. Alberto and M. Fraga, *Journal of Medicinal Chemistry,* **28**, 238(2023), https://doi.org/ 10.3390/molecules28020838
16. M. Maneeta Devi, K. Subharani Devi, O. Mukherjee Singh and T. Prasanta Singh, *Journal of Heterocyclic Communications,* **8**, 872(2024), https://doi.org/10.1515/hc-2022-0173
17. Y. Zhang, F. Tang, X. He, C. Wang, L. Kong, J. Yang and A. Diny, *Crystal Engineering Communications,***24**, 6865(2022), https://doi.org/10.1039/D2CE00953F
18. A.Y. Usyatinsky and Y.L. Khmelnitsky, *Tetrahedron Letters,* **41**, 5031(2000), https://doi.org/10.1016/S0040-4039(00)00771-1
19. Y. He, Y.Z. Chen, H.W. Du, L.A. Schmid and C.J. Lovely, *Tetrahedron Letters,***45**, 5529(2004), https://doi.org/10.1016/j.tetlet.2004.05.011
20. D. A. Shabalin and E. C. Jason, *Organic & Biomolecular Chemistry,***18,** 3950(2020), https://doi.org/10.1039/Do0B00350F
21. A. Assadieskandar, M. Amini, M. Salehi, H. Sadeghian, M. Alimardani, A. Sakhteman, H. Nadri and A. Shafiee, *Bioorganic Medicinal Chemistry,***20**, 7166(2012), https://doi.org/10.3390/molecules23030685
22. H.V. Tolomeu and C.A. Manssour Fraga, *Molecules,* **28**, 838(2023), https://doi.org/10.3390/molecules 28020838
23. S.A. Laufer, W. Zimmermann and K.J. Ruff, *Journal of Medicinal Chemistry,***47**, 6311(2004), https://doi.org/10.1021/jm0496584
24. S. Rualhania, S. Kumar, B. Nehra, G.D. Gupt and V. Monga, *Journal of Medicinal Chemistry,* **1232**,129982(2021), https://doi.org/10.1016/j.molstruc.2021.129982
25. C. Congiu, M.T. Cocco and V. Onnis, *Bioorganic & Medicinal Chemistry Letters*, ,**18,** 989(2008), https://doi.org/10.1016/j.bmcl.2007.12.023
26. B.F. Abdel Wahab, E.A. Ghada and F.A. Badria, *European Journal of Medicinal Chemistry,* **46,** 1501(2011), https://doi.org/10.1016/j.ejmed.201.01.062
27. Verma Garima, Manella Akranth, Shaquiquzzaman, Mohammad Akhtar, Mymoona Ali, Mohammad Rahmat, and Mohamad Mumtaz, *Journal of Pharmacy and Bioallied Sciences,* **6,** 69(2014), https://doi.org/10.4103/0975-7406.129170
28. XM Peng, GX Cai, CH Zhou, *Current Topics in Medicinal Chemistry*, **13,** 125(2013), https://doi.org/10.2174/15680266113139990125
29. A.S. Leutou, I. Yang, H. Kang, E.K. Seo, S.J. Nam and W. Fenical, *Journal of Natural Products,***78(11),** 2846(2015), https://doi.org/10.1021/acs.jnatprod.5b00746
30. Pingwu, Xueguozhang and Baohuachen, *Tetrahedron Letters*, **60,** 1103(2019), https://doi.org/10.1016/j.tetlet.2019.03.025
31. M.J. Frisch, G.W. Trucks, H.B. Schlegel, G.E. Scuseria, M.A. Robb, J.R. Cheeseman, J.A. Montgomery, J.M. Vreven, V. Iyengar, V.G. Mennucci, S.C. Dapprich and J.A. Pople, *Gaussian Inc.,* **67,** 810020(2004), https://doi.org/10.4236/jemaa.2016.810020
32. Y. Hua and C. Yu, *European Journal of Medicinal Chemistry,* **269,** 116278(2024), https://doi.org/10.1016/j.ejmech
33. F. Wan, H. Shi, W. Chen, Z. Gu, L. Du, P. Wang, J. Xin Wang and Y. Hung, *Nanomaterial,***7,** 210(2017), https://doi.org/10.3389/fmolb.2020.00193
34. T. Mosmann, *Journal of Immunological Methods*, **65,** 63(1983), https://doi.org/10.1016/0022-1759(83) 90303-4
35. S.J. Gawandi, V.G. Desi, S. Joshi, S. Shingade and R.R. Pissurlenkar, *BioOrganic Chemistry*, **117,** 105331(2021), https://doi.org/10.1016/j.bioorg.2021.105331

36. D. Rajaraman, G. Sundararajan, N.K. Loganath and K. Krishnasamy, *Journal of Molecular Structure*, **1127,** 610(2017), https://doi.org/10.1016/j.molstruc.2016.08.021
37. J. Jayabharathi, V. Thanikachalam and M. Venkatesh Perumal, *Spectro Chemica Acta Part A.,* **85,** 37(2012), https://doi.org/10.11071s2053229617002522
38. J.P. Foster and F. Wienhold, *Journal of American Chemical Society,* **102(24),** 7211(1980), https://doi.org/10.1021/ja00544a007
39. J. Chocholousova, V. Spirko and P. Hobza, *Physical Chemistry Chemical Physics*, **6,** 41(2004), https://doi.org/10.1021/jp208270u
40. M. Alcolea Palafox, *Journal of Physical Chemistry A,* **103,** 11377(1999), https://doi.org/10.1021/jp990591j

[RJC-9138/2025]